

2-Oct-24

1 **Fluorescent Antibody-Based Detection and Ultrastructural Analysis of *Streptococcus***
2 ***pneumoniae* in Human Sputum**

3
4 Ana G. Jop Vidal^{1,#}, Meg Francis^{1,#}, Maneesha Chitanvis⁴, Ithiel J. Frame^{3,*}, Poonam Sharma³,
5 Patricio Vidal¹, Claudio F. Lanata⁵, Carlos Grijalva⁶, William Daley³, and Jorge E. Vidal^{1,2}

6
7 ¹Department of Cell and Molecular Biology, ²Center for Immunology and Microbial Research,
8 ³Department of Pathology, University of Mississippi Medical Center, Jackson MS; ⁴Rollins School
9 of Public Health; Emory University, Atlanta GA; ⁵Instituto de Investigacion Nutricional; Lima,
10 Peru; ⁶Department of Health Policy, Vanderbilt University Medical Center, Nashville, TN

11
12 #These authors contributed equally to the manuscript

13 *Current affiliation: Quest Diagnostics, Lewisville, TX

14
15 Running title: Spn-FLUO for pneumococcal detection in sputum

16
17 Address correspondence to:

18 Jorge E. Vidal, PhD. Department of Cell and Molecular Biology, University of Mississippi Medical
19 Center. 2500 North State St, Jackson MS 39216. Email: jvidal@umc.edu

20
21

2-Oct-24

22 Abstract

23 **Background:** Pneumococcal pneumonia continues to be a significant global health burden,
24 affecting both children and adults. Traditional diagnostic methods for sputum analysis remain
25 challenging. The objective of this study was twofold: to develop a rapid and easy-to-perform
26 assay for the identification of *Streptococcus pneumoniae* (Spn) directly in sputum specimens
27 using fluorescence microscopy, and to characterize with high-resolution confocal microscopy
28 the ultrastructure of pneumococci residing in human sputum. **Methods:** We fluorescently
29 labeled antibodies against the pneumococcal capsule (Spn-FLUO). The specificity and sensitivity
30 of Spn-FLUO for detecting Spn was evaluated *in vitro* and *in vivo* using mouse models of
31 carriage and disease, human nasopharyngeal specimens, and sputum from patients with
32 pneumococcal pneumonia. Spn was confirmed in the specimens using culture and a species-
33 specific qPCR assays. Confocal microscopy and Imaris software analysis were utilized to resolve
34 the ultrastructure of pneumococci in human sputum. **Results:** Compared with cultures and
35 qPCR, Spn-FLUO demonstrated high sensitivity (78-96%) in nasopharyngeal samples from mice
36 and humans. The limit of detection (LOD) in nasopharyngeal samples was $\geq 1.6 \times 10^4$ GenEq/ml.
37 The specificity in human nasopharyngeal specimens was 100%. In lung specimens from mice
38 infected with pneumococci, Spn-FLUO reached 100% sensitivity with a LOD of $\geq 1.39 \times 10^4$
39 GenEq/ml. In human sputum, the sensitivity for detecting Spn was 92.7% with a LOD of 3.6×10^3
40 GenEq/ml. Ultrastructural studies revealed that pneumococci are expectorated as large
41 aggregates with a median size of $1336 \mu\text{m}^2$. **Conclusions:** Spn-FLUO is a rapid and sensitive
42 assay for detecting Spn in human sputum within 30 min. The study highlights that most
43 pneumococci form aggregates in human sputum.

2-Oct-24

2-Oct-24

45 **Background**

46 *Streptococcus pneumoniae* (Spn) strains infect the lungs causing pneumococcal
47 pneumonia, a common community-acquired pneumonia (CAP) that causes over a million
48 deaths annually worldwide¹. Pneumococcal pneumonia is an acute bacterial infection of the
49 pulmonary parenchyma caused by colonization of the lung and subsequent, or concurrent,
50 invasion of pneumococci into the respiratory epithelium^{2, 3}. Invasion of bronchi and terminal
51 bronchiole leads pneumococci to reach respiratory bronchiole, alveolar ducts, and alveoli,
52 where pneumococci have access to the alveolar-capillary network, a large surface area
53 containing ~300 billion of blood capillaries and where the exchange of CO₂ by O₂ occurs.

54 Spn strains encompass over 100 capsular types; the capsule is a target of pneumococcal
55 vaccines that have saved millions since their licensure⁴. The capsular polysaccharide is
56 negatively charged, enabling pneumococci to colonize the lungs by evading entrapment by
57 mucus secreted in the lumen of bronchi and terminal bronchiole². The capsule also acts as an
58 anti-phagocytic factor by blocking complement deposition^{2, 5, 6, 7}. Consequently, expression of
59 the pneumococcal capsule is maximized during pneumococcal pneumonia and it was utilized in
60 this study to identify the presence of Spn in clinical specimens.

61 The diagnosis of pneumococcal pneumonia is based on symptoms and suggestive
62 radiographic findings^{8, 9}. Diagnostic testing to determine pneumococcal pneumonia is optional
63 for non-hospitalized patients, while those requiring admission should undergo blood cultures,
64 respiratory cultures, and Gram staining of good-quality sputum. If the disease is severe, a
65 urinary antigen test may also be considered⁸. However, cultures have poor sensitivity and can

2-Oct-24

66 take at least 24 h to yield results. Moreover, the urinary antigen test for identifying
67 pneumococcal pneumonia has limited sensitivity and specificity⁸.

68 Pneumonia multiplex (m)PCR panels have demonstrated superior performance in
69 detecting respiratory pathogens, including pneumococcal strains. mPCR panels offer improved
70 specificity and turnaround time compared to traditional methods¹⁰. Other molecular assays
71 include real-time PCR methods targeting a number of species-specific genes, or gene
72 sequences, such as the gene encoding the autolysin *lytA*^{11, 12}, the pneumolysin *ply*¹² gene, the
73 permease gene *piaB* of the iron transporter PiaABC¹³ or a putative transcriptional regulator
74 SP2020¹⁴. These PCR assays typically exhibit high sensitivity and specificity (>90%), and
75 depending on the platform, real-time assays can deliver results within 3-4 h.

76 Prompt and accurate identification of pneumococcal pneumonia as the etiology is
77 crucial for tailoring antibiotic management to a specific patient, which is paramount to
78 preventing complications and mortality^{8, 15}. Early administration of antibiotic therapy has been
79 demonstrated to improve short-term mortality rates in both human patients and animal
80 models of pneumococcal disease^{16, 17}. Antibiotic therapy for community-acquired pneumonia
81 (CAP) is typically initiated empirically within 1-2 h of presentation to a healthcare facility, prior
82 to the identification of the causative pathogen¹⁶. However, the indiscriminate use of empirically
83 prescribed antibiotics has contributed to a significant increase in antimicrobial resistance rates,
84 particularly in certain geographical regions. For example, in some areas, over 70% of Spn strains
85 isolated from pneumococcal pneumonia cases are resistant to first-line macrolide antibiotics¹⁸,
86 ¹⁹.

2-Oct-24

87 Addressing the global burden of antibiotic resistance requires multifaceted efforts,
88 including ensuring equitable access to, and developing innovative, diagnostics. In this study, we
89 fluorescently labeled antibodies against the pneumococcal capsule, hereafter referred to as
90 Spn-FLUO, and evaluated their performance in detecting pneumococcal strains within 30 min.
91 Given the capsule's high expression during pneumococcal disease, we hypothesized that
92 antibodies targeting the capsule would enhance the rapid detection of strains in lower airway
93 specimens. We systematically tested Spn-FLUO to detect Spn strains grown *in vitro*, as well as
94 strains colonizing the upper and lower airways of mice in murine models of carriage and
95 disease. Additionally, we assessed the efficacy of Spn-FLUO in detecting Spn strains colonizing
96 the nasopharynx of children. We evaluated the diagnostic performance of Spn-FLUO in
97 identifying pneumococcal pneumonia as the etiology in specimens collected from patients with
98 pneumococcal pneumonia. Results were obtained within 30 min of sample collection.

99 Given the distinctive characteristics of the pneumococci observed in the sputum, we
100 conducted additional ultrastructural studies using high-resolution laser scanning confocal
101 microscopy and advanced image analysis. Consequently, we present novel insights into the
102 ultrastructure of pneumococcal aggregates formed in human sputum.

103

104 **Methods**

105 **Bacterial strains, culture media, and antibiotics.** Spn reference strains and mutants used in the
106 present study were: TIGR4²⁰, SPJV41^{21, 22}, D39²³, EF3030²⁴, S19F 4924²⁵ and S6B 8655²⁶. Strains
107 were routinely cultured on blood agar plates (BAP), or grown in Todd Hewitt broth containing
108 0.5% (w/v) yeast extract (THY), at 37°C with a 5% CO₂ atmosphere. Where indicated,

2-Oct-24

109 streptomycin (Str, 200 µg/ml), trimethoprim (Tmp, 10 µg/ml), tetracycline (Tet, 1 µg/ml),
110 or/and erythromycin (Ery, 1 µg/ml) was added to BAP. All antibiotics were purchased from
111 Millipore-Sigma Sigma-Aldrich.

112 **Preparation of inocula.** The inoculum was prepared as previously described²⁷. Briefly, bacteria
113 were inoculated on blood agar plates (BAP) and incubated overnight at 37°C in a 5% CO₂
114 atmosphere. Bacteria were then harvested from plates by PBS washes and this suspension was
115 used to inoculate THY or cell cultures, that was brought to a final OD₆₀₀ of ~0.1. This suspension
116 contained ~5.15x10⁸ cfu/ml as verified by serial dilution and plating of aliquots of the
117 suspension.

118 **Cell cultures.** Human pharyngeal Detroit 562 cells (ATCC CCL-138) were cultured in Eagle's
119 minimum essential medium (MEM) (Gibco) supplemented with non-heat-inactivated 10% fetal
120 bovine serum (FBS) from R&D systems, 1% nonessential amino acids (Gibco), 1% glutamine
121 (Gibco), penicillin (100 U/ml), and streptomycin (100 µg/ml), and the pH was buffered with
122 HEPES (10 mM) (Gibco). Cells were harvested with 0.25% trypsin (Gibco), resuspended in the
123 cell culture medium, and incubated at 37°C in a 5% CO₂ humidified atmosphere.

124 **Fluorescent labeling of anti-capsule antibodies.** Antibodies were purchased from the Statens
125 Serum Institute (Denmark). The following antibodies were used throughout this study: Omni
126 antiserum (recognizes 92 serotypes), type serum 2, type serum 4, group serum 6, and group
127 serum 19. Serum was depleted of proteins less than 100 kDa using an Amicon Ultra-100K
128 centrifugal filter (Millipore-Sigma), washed three times with PBS. Proteins were quantified using
129 Bradford reagent, and 1 mg of the antibodies was labeled with either Alexa-488 or Alexa-555
130 following the manufacturer's recommendations (Molecular Probes). After purification by size

2-Oct-24

131 exclusion chromatography (≥ 40 kDa), collected fractions were assessed for reactivity against
132 the specific serotype, serogroup, or several serotypes for the Omni antiserum. Proteins were
133 quantified from reactive fractions using the Bradford assay, and antisera were stored at 4°C for
134 short-term or -20°C for long-term storage. Labeled antibodies stored at 4°C remained reactive
135 for up to three months, while those frozen have been effective in labeling bacteria for over
136 three years. For the sake of simplicity, the fluorescently labeled Omni antiserum is referred to
137 as Spn-FLUO throughout this manuscript.

138 ***In vitro* imaging of pneumococci.** Pneumococci were inoculated into 8-well glass slides (Lab-
139 Tek[®]) and incubated for 4 h at 37°C in a 5% CO₂ atmosphere. Some slides contained cultures of
140 Detroit 562 cells (ATCC CCL-198) grown to confluence, typically 7 days post seeding.
141 Pneumococci attached to the glass substratum or human cells were then washed twice with
142 PBS and fixed with 2% PFA for 15 min at room temperature. After removing the 2% PFA, the
143 bacteria were washed with PBS and blocked with 2% bovine serum albumin (BSA) for 1 h at
144 37°C. The pneumococci were then incubated with the specified labeled antibodies (~20 µg/ml)
145 for 1 h at room temperature. The stained preparations were subsequently washed twice with
146 PBS and mounted with ProLong Diamond Antifade Mountant with DAPI (Molecular Probes). In
147 some preparations, DAPI was replaced with TO-PRO-3 (1 µM), a carbocyanine monomer nucleic
148 acid stain (Molecular Probes). Fluorescence images were acquired using an upright, epi-
149 fluorescence Nikon Ni-U Research Microscope equipped with a Nikon DS-Qi2 sCMOS Camera
150 system. Confocal images were obtained using a Nikon C2 laser scanning confocal microscopy
151 system, and the micrographs were analyzed with ImageJ version 1.49k (National Institutes of
152 Health, USA) or Imaris software (Bitplane).

2-Oct-24

153 **Mouse models of pneumococcal nasopharyngeal carriage and disease.** Inbred 6-7 week-old
154 C57BL/6 mice -pneumococcal carriage-, or 4-5 week-old Balb/c mice -pneumococcal
155 pneumonia- model (Charles River Laboratories) were anesthetized with 5% isoflurane (vol/vol)
156 in oxygen (2 liters/min) administered via an RC2 calibrated vaporizer (VetEquip Inc) and then
157 infected with $\sim 1 \times 10^5$ CFU of strain Spn EF3030 (carriage model) or $\sim 1 \times 10^8$ cfu of TIGR4 or
158 SPJV41 (pneumonia model). The animals were weighed daily, and their behavior and
159 appearance were monitored twice daily for up to four days. Mice in the pneumonia model were
160 euthanized when they lost $\geq 20\%$ of their body weight, compared to their body weight before
161 infection, or when mice were non-responsive to manual stimulation, and/or if they show signs
162 of illness such as ruffled fur, intermittent hunching, and exhibiting respiratory distress. Mice
163 were then euthanized, and the upper airways, including nasopharyngeal tissue or the lungs,
164 were aseptically collected, placed in THY with 10% glycerol and immediately homogenized. For
165 fluorescence staining (explained below), the nasopharynx from some mice was collected and
166 fixed with 10% PFA. The specimens were then stored at -80°C . This aliquot was used for
167 bacterial counts and detection with labeled antibodies. To obtain bacterial counts, the
168 homogenized tissue was serially diluted in PBS and plated onto BAP with gentamicin. The
169 Institutional Animal Care and Use Committee (IACUC) at the University of Mississippi Medical
170 Center approved the protocol used in this study (1584), overseeing the welfare, well-being, and
171 proper care of all mice utilized in this study. All mouse experiments followed the guidelines
172 outlined in the National Science Foundation Animal Welfare Act (AWA).

173 **Fluorescence staining of nasopharyngeal tissue.** The PFA-fixed nasopharynxes were paraffin-
174 embedded, sectioned ($\sim 5 \mu\text{m}$), mounted on a slide and deparaffinized. Tissues were washed

2-Oct-24

175 three times with PBS and the preparations were blocked with 2% bovine serum albumin (BSA)
176 for 1 h at room temperature. These preparations were then incubated for 1 h with serogroup-
177 specific (S19) polyclonal antibody (Statens Serum Institute, Denmark) (20 µg/ml) that had been
178 previously labeled with Alexa-555 (Molecular Probes). Stained tissues were finally washed three
179 times with PBS, air dried and then mounted with ProLong Diamond Antifade mounting medium
180 containing DAPI (Molecular Probes). Confocal micrographs were obtained using a Nikon C2
181 laser scanning confocal microscopy system and analyzed using the Imaris software (Bitplane).

182 **Specimens from Humans with Pneumococcal Pneumonia.** Human specimens, including
183 sputum and bronchoalveolar lavages from de-identified patients with microbiologically and
184 radiologically confirmed pneumococcal pneumonia, were utilized in this study. Institutional
185 Review Board (IRB) exemption was obtained for the use of these de-identified specimens.
186 When available, the age of the patients ranged from 19 months through 60 years. The
187 specimens were collected according to institutional guidelines by the University of Mississippi
188 Medical Center's clinical laboratory and stored at -80°C until processed. As part of the
189 microbiological diagnostics, the pathology laboratory at UMMC isolated a Spn strain from each
190 specimen. Additionally, the Spn etiology was confirmed by *lytA*-based real-time PCR, as
191 detailed^{28, 29} and briefly described below.

192 **Human nasopharyngeal specimens.** Human nasopharyngeal specimens (N=50) utilized in the
193 current study had been collected from Peruvian children and processed for pneumococcal
194 detection and quantification by qPCR and culture in previous studies^{30, 31}. Children enrolled in
195 the mentioned studies were aged 0-3 years of age; details on the study population have been
196 published elsewhere^{31, 32, 33}. De-identified specimens were processed at Emory University,

2-Oct-24

197 obtaining IRB exemption. Briefly, these nasopharyngeal samples were collected following WHO
198 recommendations³⁴ with a deep NP swab, using rayon polyester swabs and were immediately
199 placed in 2.0 ml cryogenic vials with 1 ml of transport medium, a mixture containing skim milk-
200 tryptone-glucose-glycerin (STGG) and then stored at -80°C³⁵.

201 **Identification of pneumococcus using Spn-FLUO in mouse tissue or human specimens.**

202 Specimens were thawed on ice and an aliquot (10 µl) of each specimen was immediately mixed
203 with Spn-FLUO (50 µg/ml) and incubated for 10 min at room temperature in the dark. Five µl of
204 this suspension was dropped onto a microscope slide and covered with a coverslip. The stained
205 sample was analyzed within five minutes using an upright, epi-fluorescence Nikon Ni-U
206 Research Microscope equipped with a Nikon DS-Qi2 sCMOS Camera system. We first situated
207 the specimen in the correct optical plane (i.e., visualizing cells, tissue, and/or bacteria) with the
208 60x objective and a bright light source. The slides were then analyzed and scored using
209 epifluorescence in the green channel, following a semiquantitative algorithm: 1-5 pneumococci
210 per field in at least three fields corresponded to “+”, 5-10 pneumococci per field to “++”, and
211 more than 10 pneumococci per field was scored as “+++”. Negative samples had no
212 pneumococci observed. Micrographs from positive specimens were obtained using the 60x and
213 100x objectives.

214 **Staining and confocal analysis of human sputum.** An aliquot of sputum sample (10 µl) was
215 dropped onto a slide and air dry for ~20 min at room temperature. The sputum was then
216 stained for 1 h with Spn-FLUO (20 µg/ml) and wheat germ agglutinin conjugated to Alexa-555
217 [(WGA), 5 µg/ml]. The stained specimen was washed three times with PBS, air-dried, and
218 mounted with ProLong Diamond Antifade mounting medium containing DAPI (Molecular

2-Oct-24

219 Probes). Confocal micrographs were obtained using a Nikon C2 laser scanning confocal
220 microscopy system and z-stacks micrographs were analyzed using the NIS Elements Basic
221 Research software, version 4.30.01 build 1021. For 3D visualization, creation of animations, and
222 quantification purposes, images were processed using the Imaris software 64x Version 10.1.0
223 (Oxford Instruments).

224 **DNA extraction and quantitative PCR (qPCR).** DNA was extracted as described earlier using a
225 QIAamp DNA mini kit (Qiagen)^{30, 36}. Bacterial density was quantified by qPCR reactions in a total
226 25 μ l volume. Reactions contained 1x Platinum qPCR superMix (Invitrogen), 200 nm each of
227 primers and probe, and 2.5 μ l of purified DNA. The nucleotide sequence of primers and probe
228 were published elsewhere¹². No template controls (NTC) were run with each set of samples.
229 qPCR reactions were carried out using a CFX96 Real-Time PCR Detection System (Bio-Rad). The
230 following amplification parameters were utilized, 95°C for 2 min, followed by 40 cycles of 95°C
231 for 15 s and 60°C for 1 min. qPCR standards using genomic DNA from reference strain TIGR4
232 (ATCC BAA-334) were run in parallel to construct a standard curve utilized to calculate genome
233 equivalents (GenEq)/ml using the software Bio-Rad CFX manager. Standards DNA Preparation:
234 Purified DNA was adjusted to a concentration of 1 ng/ μ l in TE buffer (10 mM Tris-HCl, 1 mM
235 EDTA, pH 8.0) and immediately stored at -80°C until use. Standards for quantification were
236 prepared within an hour before reactions by serially diluting a 1 ng/ μ l aliquot in TE buffer to
237 final concentrations of 100 pg/ μ l, 10 pg/ μ l, 1 pg/ μ l, 100 fg/ μ l, 50 fg/ μ l, and 5 fg/ μ l of
238 pneumococcal DNA. Given the 2.1608 Mb genome size of TIGR4²⁰, these standards
239 corresponded to 4.29×10^5 , 4.29×10^4 , 4.29×10^3 , 4.29×10^2 , 4.29×10^1 , 2.14×10^1 , or 2.14 GenEq,

2-Oct-24

240 respectively. Standards prepared using this protocol consistently achieved an efficiency greater
241 than 90% throughout the study (data not shown).

242

243 **Isolation and identification of *S. pneumoniae* strains.** Nasopharyngeal specimens were
244 thawed, vortexed for 15 s and 200 µl transferred to a 5 ml Todd-Hewitt broth (THY) containing
245 0.5% of yeast extract and 1 ml of rabbit serum (Gibco® by Life Technologies)³⁷. This enriched
246 culture was incubated for 6 h at 37°C in a 5% CO₂ atmosphere and then inoculated onto BAP
247 and incubated for 18-24 h at 37°C in a 5% CO₂ atmosphere. Spn strains were isolated and
248 identified using the optochin test (Remel) and bile solubility test as previously described³⁷.

249 Spn strains were isolated and identified from lower respiratory tract specimens
250 including sputum, endotracheal aspirates, bronchoalveolar lavage fluids, bronchial washings,
251 protected brush specimens, and lung aspirates, using standard methodologies³⁸. Briefly, after
252 Gram staining, the primary media including 5% Columbia sheep blood, Chocolate, and
253 MacConkey agars (BD BBL™) were inoculated. Thioglycolate broth was employed for bronchial
254 brush samples. The media were incubated for 18 to 24 h at 35-37°C in 5% CO₂, and cultures that
255 remained negative after this period were re-incubated for another 24 h.

256 Pathogenic organisms were identified and susceptibility testing was performed only on
257 significant growth, characterized by moderate to abundant colonies in the second or further
258 quadrants of the plate, small numbers of a pathogen consistent with the predominant Gram-
259 stain morphotype, and associated with inflammatory white blood cells, or colonies in the first
260 quadrant if minimal or no other normal flora was present. Alpha-hemolytic, dry, or mucoid
261 colonies resembling Spn strains were identified using Matrix Assisted Laser Desorption

2-Oct-24

262 Ionization Time-of-Flight (VITEK[®] MS) or VITEK[®] 2 Gram-Positive identification card (GP), and
263 purity was confirmed with the optochin disc. The antibiotic sensitivity was determined using
264 VITEK[®] 2 Gram-Positive Susceptibility Cards, and the manual D-test.

265 **Statistical analysis.** We performed one-way analysis of variance (ANOVA) followed by Dunnett's
266 multiple-comparison test when more than two groups were compared or Student's t test to
267 compare two groups, as indicated. All statistical analysis was performed using the software
268 GraphPad Prism (version 8.3.1).

269

270 **Results**

271 ***In vitro* assessment of fluorescently-labeled anti-Spn antibodies for detecting *S. pneumoniae***
272 **strains.** We first evaluated the ability of fluorescently-labeled antibodies to detect specific Spn
273 strains. Antibodies targeting vaccine serotypes, or serogroups, were labeled as detailed in
274 Material and Methods. In addition to their specific reactivity against corresponding
275 serotypes/serogroups, the labeled antibodies did not exhibit cross reactivity against a panel of
276 other serotypes (not shown). For instance, the anti-S4-A488 (green), or anti-S19-A555 (red)
277 antibody specifically stained Spn serotype 4 or 19F, respectively, within five min of exposure as
278 evaluated by fluorescence microscopy (**Fig. 1A and not shown**). High-resolution micrographs
279 using confocal microscopy were obtained from S19F strain 4924 growing on a glass substratum
280 (**Fig. 1B**).

281 We next evaluated the detection of Spn strains using fluorescently labeled antibodies in
282 strains infecting *in vitro*-cultured human pharyngeal cells. Pharyngeal cells were infected for
283 four h with strain D39 (serotype 2) or with a mixture of strains D39 and TIGR4 (serotype 4), and

2-Oct-24

284 subsequently stained with anti-S2-A555 or with a combination of anti-S2-A555 and anti-S4-
285 A488. Cell nuclei were also stained with a fluorescent dye. Spn strains were identified in cells
286 infected with a single serotype (Fig. 1C). Additionally, each individual Spn strain was detected
287 on pharyngeal cells infected with the D39-TIGR4 mixture (Fig. 1D).

288

289 **Detection of Spn vaccine strain serotype 19F in the mouse upper respiratory tract.** A murine
290 model of nasopharyngeal carriage was employed to assess the utility of fluorescent antibodies
291 for detecting Spn strains. Eleven mice were intranasally inoculated with $\sim 10^5$ colony-forming
292 units (CFU) of Spn strain EF3030, a serotype 19F strain commonly used in animal models of
293 pneumococcal carriage^{24, 39}. This inoculum was previously optimized to induce colonization
294 levels comparable to those observed in the nasopharynx of children^{33, 40}.

295 Two days post-infection, nasopharyngeal tissue from the upper respiratory tract was
296 collected and stored in paraformaldehyde or homogenized. An aliquot of the nasopharyngeal
297 homogenate was subjected to serial dilution and plating to quantify the pneumococcal burden.
298 All mice were colonized with a median bacterial load of 7.2×10^4 cfu/organ (interquartile range:
299 7.1×10^4 - 3.3×10^5) (Table 1). Subsequently, aliquots of the nasopharyngeal homogenates were
300 subjected to pneumococcal detection assays. We employed an anti S19-A555 antibody, known
301 to recognize strain serotype 19F EF3030⁴¹, and Spn-FLUO antibody raised against 92
302 pneumococcal serotypes, including serotype 19F. Both antibodies detected pneumococci in
303 72% of the specimens (8/11) (Fig. 1E and Table 1). Detection of pneumococci was not achieved
304 in nasopharyngeal homogenates with a bacterial density $\leq 7.1 \times 10^3$ cfu/organ (Fig. 1G and Table
305 1). Histological analysis of nasopharyngeal tissue revealed intracellular pneumococci within

2-Oct-24

306 goblet cells indicating a good performance of antibody-based detection at the tissue level (Fig.
307 1F).

308

309 **Phenotypic and genotypic identification of *S. pneumoniae* in human nasopharyngeal**
310 **specimens.** For this initial proof-of-concept study, we selected fifty nasopharyngeal specimens
311 from children from our previous studies^{28, 30, 42} and were divided into two groups (N=25 each) as
312 detailed in Table 2. In one group, containing nasopharyngeal specimens listed as 1 through 25,
313 Spn strains were isolated and identified using both traditional and genomic methods. In the
314 other group (i.e., nasopharyngeal specimens 26 through 50) Spn cultures were negative.

315 DNA was extracted from these nasopharyngeal samples and utilized as template in qPCR
316 reactions targeting the species-specific *lytA* gene. Nasopharyngeal specimens 26 through 50
317 tested negative for Spn using *lytA*-PCR. As expected, *lytA*-PCR was positive for all
318 nasopharyngeal specimens 1 to 25 (Table 2). The specimens were processed microscopically
319 using fluorescently labeled antibodies, following the algorithm outlined in Figure 2A. Five
320 distinct fields were examined within each preparation. The sensitivity of Spn-FLUO for detecting
321 Spn strains in human nasopharyngeal specimens was 96% (24/25), while specificity was 100%
322 as no Spn was detected in *lytA*-negative, culture-negative specimens. A typical microscopy
323 finding from specimens containing abundant Spn (i.e., +++) is shown in Fig. 2C-D. The lowest
324 bacterial density detected by fluorescent antibody staining was 1.61×10^4 GenEq/ml (Table 2
325 and Fig. 2B).

326

2-Oct-24

327 **Detection and quantification of *Streptococcus pneumoniae* in mouse lung tissue during**
328 **pneumonia.** We next conducted a pre-clinical evaluation of Spn-FLUO for the detection of
329 pneumococci in lung specimens using a murine model of pneumococcal pneumonia. Mice were
330 infected with Spn strain TIGR4 and euthanized when moribund. Lungs were collected,
331 homogenized, and the Spn bacterial load was determined by serial dilution and plating (Table
332 3). Lungs from mice infected with an isogenic capsule-deficient mutant ($\Delta spxB\Delta ctO$) that has a
333 defect for colonization^{43, 44} served as controls. As expected, all animals infected with TIGR4
334 exhibited a high lung colonization density of 1.18×10^7 (interquartile range: 2.37×10^6 - 1.12×10^8)
335 colony-forming units (CFU)/g, whereas those infected with the isogenic mutant displayed low
336 colonization levels (Fig. 3A). Spn was detected in all lung specimens from TIGR4-infected
337 animals at varying levels of positivity. In contrast, mutant-infected animals exhibited
338 significantly lower bacterial burdens, with $< 1 \times 10^3$ cfu/g or no detectable bacteria (Fig. 3B, 3C
339 and Table 3). Specimens with the highest density and positive Spn-FLUO detection were
340 statistical different compared to those containing a lower burden of pneumococci (Fig. 3C). The
341 highest positive reaction with Spn-FLUO was achieved in lungs from mice colonized with a
342 median of 1.41×10^8 CFU/g, which was statistically significant compared to groups with lower
343 detection levels (Fig. 3B). Thus, Spn-FLUO demonstrated a strong correlation between
344 fluorescence detection of pneumococci and bacterial load in a murine model of pneumococcal
345 pneumonia, suggesting its potential as a rapid and sensitive diagnostic tool.

346

347 **Detection of pneumococcal strains using Spn-FLUO in clinical specimens from patients with**
348 **pneumococcal pneumonia.** We subsequently evaluated the sensitivity of Spn-FLUO antibodies

2-Oct-24

349 in detecting pneumococcal strains within human specimens from patients with pneumococcal
350 pneumonia. To assess this, we analyzed N=27 clinical specimens obtained from patients with
351 microbiologically confirmed pneumococcal pneumonia, each yielding a pneumococcal isolate.
352 Specimens comprised sputum and bronchioalveolar lavage fluid (Table 4). DNA was extracted
353 from all 27 specimens, each of which yielded a positive *lytA*-based qPCR result, indicating
354 varying bacterial loads expressed as genome equivalents per milliliter (GE/ml). Consistently, all
355 specimens were also positive for *piaB* (data not shown).

356 Spn-FLUO identified the pneumococcal etiology in 25/27 specimens, resulting in percent
357 positive agreement of 92.6%. Specimens with high pneumococcal detection per field using Spn-
358 FLUO contained a median bacterial load of 1.13×10^8 GE/ml by *lytA*-based qPCR (interquartile
359 range: 4.57×10^7 - 4.85×10^8) (Fig. 4A and Table 4). Specimens with low-moderate (i.e., scored +,
360 and ++) detection of Spn per field had a median bacteria load of 5.10×10^5 GE/ml (interquartile
361 range: 1.11×10^5 - 2.96×10^6), while the specimen with the lowest GE/ml that yielded a positive
362 reaction with the Spn-FLUO antibodies contained 3.63×10^3 GE/ml of pneumococcal DNA (Fig.
363 4A).

364 Representative images of Spn detected in sputum specimens are shown in Figure 4B-D.
365 Fluorescence and bright-field microscopy revealed a heterogeneous mixture of epithelial cells,
366 leukocytes, and bacteria resembling pneumococcal aggregates (Fig. 4B-D, arrows). While
367 pneumococcal chains were also observed, these were less abundant than the bacterial
368 aggregates. In a sputum specimen from a patient with pneumococcal pneumonia, additional
369 bacteria were noted, although only pneumococci were stained by Spn-FLUO (Figure 4B-D,

2-Oct-24

370 **arrowhead**). In summary, Spn-FLUO detected Spn strains in 92.6% of clinical specimens from
371 patients with pneumococcal pneumonia within 30 min.

372

373 **Ultrastructural studies of *Streptococcus pneumoniae* in human sputum.** Given the presence of
374 abundant mucus and thick smears in some specimens, as well as the observation of large
375 pneumococcal aggregates in unprocessed sputum, we performed high-resolution 3D confocal
376 analysis of sputum specimens. Sputum was stained with Spn-FLUO, DAPI, and wheat germ
377 agglutinin (WGA which binds to N-acetyl-D-glucosamine (GlcNAc) and sialic acid (SA) residues.
378 GlcNAc/SA was utilized since sialic acid is a biomarker for mucin content⁴⁵. A middle optical
379 section of the XY, XZ (bottom panel), and YZ (side panel) focal planes revealed a large structure
380 composed of aggregated pneumococci, isolated smaller aggregates, and pneumococcal chains
381 (**Fig. 5A and Video S1**). An optical zoom revealed abundant DNA located adjacent to
382 pneumococcal aggregates, suggesting the release from neighboring cells or cellular lysis (**Fig.**
383 **5B**). Orthogonal XZ and YZ sections demonstrated that the aggregates were embedded within
384 the sputum (**Fig. 5B, bottom panel**). Pneumococci in closed proximity to cell nuclei, either in the
385 process of capsule loss or already decapsulated (i.e., D-CPS), were observed in regions of the
386 sputum resembling internalized bacteria (**Fig. 5C**).

387 We performed three-dimensional reconstruction of the capsule channel (green) from
388 confocal z-stacks (**Fig. 5D**) and categorized pneumococci into two groups: those within
389 aggregates (**Fig. 5E**) and those forming chains or dispersed within the preparation (**Fig. 5F**).
390 Representative pneumococcal aggregates are shown in **Fig. 5G**. The area of these
391 pneumococcal aggregates was significantly different compared to all other pneumococci (**Fig.**

2-Oct-24

392 **5H**). The median area of pneumococcal aggregates was $1336 \mu\text{m}^2$ (interquartile range: 959 –
393 $2108 \mu\text{m}^2$) whereas the median area of pneumococcal chains and dispersed bacteria was 9.15
394 μm^2 (interquartile range: $3.6 - 14.3 \mu\text{m}^2$) (**Fig. 5G**).

395 Further 3D analysis of orthogonal XY and XZ focal planes demonstrated that the
396 GlcNAc/SA signal did not colocalize with pneumococcal aggregates but instead surrounded
397 encapsulated pneumococci (**Fig. 5I**). Overall, the data revealed that pneumococcal aggregates
398 embedded in sputum specimens are significantly larger than those in chain or dispersed forms,
399 potentially providing a physical barrier shielding pneumococci from sputum components.

400

401 **Discussion**

402 In this study, we demonstrated the feasibility of fluorescent antibody-based microscopy
403 for the rapid diagnosis of pneumococcal pneumonia. The entire process, from sample collection
404 to final diagnosis, was completed within 30 min. Prompt identification of the causative agent is
405 crucial in severe pneumonia, often influencing patient outcomes⁹. Spn-FLUO offers a valuable
406 alternative for rapid diagnosis, particularly in cases where mortality remains high despite low
407 antibiotic resistance rates, as observed with serotype 3 strains in Spain⁴⁶. The rapid
408 identification of the pneumococcus in clinical specimens allows for timely adjustment of
409 empirical therapy, which is particularly important in severe cases. Although this technology
410 requires a fluorescence microscope, the objective nature of the fluorescent signal from Spn
411 strains makes fluorescence antibody-based detection suitable for resource-limited regions, as
412 DNA extraction, reaction mixtures, and real-time systems are not necessary, and minimal
413 training is required. Furthermore, clinical trials recruiting patients with pneumococcal

2-Oct-24

414 pneumonia can benefit from a swift decision on whether potential individuals with signs and
415 symptoms of pneumococcal pneumonia can be included in the trial.

416 Despite significant advancements in technology for the detection of pathogens causing
417 pneumonia, pneumococcal pneumonia diagnosis remains challenging⁹. The culture of lower
418 respiratory tract specimens, while considered the gold standard, is often associated with delays
419 and low sensitivity. Multiplexed PCR panels have demonstrated improved sensitivity to detect
420 pathogens not recovered by culture, but they require substantial resources, specialized
421 equipment, and highly trained personnel, with turnaround times of several hours^{9, 10, 47}. Antigen
422 detection assays, such as those targeting the pneumococcal capsule, offer the advantage of
423 rapid turnaround time. However, their specificity to a single pathogen represents a limitation.
424 Nonetheless, they can be a life-saving tool in critical situations.

425 To the best of our knowledge, no previous studies have investigated the ultrastructure
426 of pneumococci in freshly expectorated human sputum from patients with pneumonia. The
427 current study filled this gap by characterizing the unique structures formed by pneumococci in
428 the sputum. These bacterial aggregates are large, with a median size of 1336 μm^2 , and have not
429 been observed invading the lungs of patients with pneumococcal pneumonia or in the lungs of
430 mice infected with Spn strains. This population of pneumococci, which likely resides
431 extracellularly on bronchi and bronchioles, may be formed to resist the innate and adaptive
432 immune response. These aggregated extracellular pneumococci represent an important novel
433 population that may be more resistant to antibiotics and antimicrobial peptides.

434 Our study has some limitations. Notably, Spn-FLUO exclusively recognizes encapsulated
435 pneumococci, limiting its utility for detecting non-encapsulated strains. While the majority of

2-Oct-24

436 isolates express capsule, this limitation could hinder the detection of other non-encapsulated
437 strains⁴⁸. Additionally, studies evaluating Spn-FLUO sensitivity in both mouse lung specimens
438 and human lung specimens from patients with pneumococcal pneumonia involved specimens
439 from where strains were isolated in culture, suggesting a high bacterial load, later confirmed by
440 qPCR assays. We did not assess the specificity of Spn-FLUO against a panel of Spn-negative
441 human sputum samples or healthy subjects. Instead, as a surrogate, we utilized human
442 nasopharyngeal specimens with a *lytA*-negative reaction and lung specimens from mice
443 infected with a strain with a colonization defect and low capsule production. In both cases,
444 specificity was 100%.

445 In summary, we have characterized a rapid method for detecting the pneumococcus in
446 clinical specimens from patients with pneumonia. Using the fluorescent antibodies developed
447 in this study, we have provided novel ultrastructural information regarding a previously
448 uncharacterized population of pneumococcal aggregates. This study serves a dual purpose.
449 First, antibody-based detection of pneumococci can be further developed to guide empirical
450 therapy while awaiting culture results. Second, it fosters novel research into pneumococcal
451 aggregates, which may serve as reservoirs for the pneumococcus.

452

453 **List of abbreviations**

454 *Streptococcus pneumoniae*: Spn

455 Fluorescent antibodies against the pneumococcal capsule: Spn-FLUO

456 Quantitative polymerase chain reaction: qPCR

457 Limit of Detection: LOD

458 Genome equivalents/milliliter: GenEq/ml

2-Oct-24

- 459 Square micrometer: μm^2
- 460 Minutes: min
- 461 Community-acquired pneumonia : CAP
- 462 Carbon dioxide: CO_2
- 463 Oxygen: O_2
- 464 Hours: h
- 465 Multiplex polymerase chain reaction: (m)PCR
- 466 Colony Forming Units: CFU
- 467 Colony forming units/gram: CFU/g
- 468 Wheat Germ Agglutinin: WGA
- 469 N-acetyl-D-glucosamine : GlcNAc
- 470 Sialic acid: SA
- 471 Blood agar plates: BAP
- 472 Todd Hewitt broth containing yeast extract: THY
- 473 Streptomycin: Str
- 474 Trimethoprim: Tmp
- 475 Tetracycline: Tet
- 476 Erythromycin: Ery
- 477 Microgram/milliliter: $\mu\text{g}/\text{ml}$
- 478 Phosphate Buffered Saline: PBS
- 479 Minimum Essential Medium: MEM
- 480 Fetal Bovine Serum: FBS
- 481 Paraformaldehyde: PFA
- 482 Bovine Serum Albumin: BSA
- 483 Micromole: μM
- 484 Institutional Animal Care and Use Committee: IACUC
- 485 National Science Foundation Animal Welfare Act: AWA

2-Oct-24

486 Institutional Review Board: IRB
487 University of Mississippi Medical Center: UMMC
488 World Health Organization: WHO
489 Nasopharyngeal: NP
490 Microliter: μ l
491 Nanogram/microliter: ng/ μ l
492 Megabase: Mb
493 Seconds: s

494

495 **Declarations**

496 **Ethics approval**

497 The research project “Mechanistic Studies of Broadly Reactive Antibodies for the
498 Treatment, Diagnosis, and Prevention of Pneumococcal Infection” has been reviewed by the
499 Institutional Review Board (IRB) of the University of Mississippi Medical Center (Federalwide
500 Assurance FWA#00003630) and has been determined to be exempt from formal review. The
501 IRB concluded that the project meets the criteria for exemption as outlined in the U. S.
502 Department of Health and Human Services Regulations for the Protection of Human Subjects,
503 45 CFR 46.102(l) because this project does not research involving human subjects. As such, no
504 additional ethical review was required.

505 All experiments involving animals were performed with prior approval of and in
506 accordance with protocol 1584 which was reviewed and approved by the UMMC Animal Care
507 Committee. UMMC laboratory animal facilities have been fully accredited by the American
508 Association for Accreditation of Laboratory Animal Care. Procedures were performed according

2-Oct-24

509 to the institutional policies, Animal Welfare Act, NIH guidelines, and American Veterinary
510 Medical Association guidelines on euthanasia.

511

512 **Consent to participate**

513 N/A

514

515 **Consent for publication**

516 N/A

517

518 **Availability of data and materials**

519 All data generated or analyzed during this study are included in this published article (and its
520 supplementary information files) and are available from the corresponding author on
521 reasonable request. The materials such as software, protocols or reagents were specified in the
522 Material and Methods section.

523

524 **Competing interests**

525 The authors declare that they have no competing interests.

526

2-Oct-24

527 **Funding**

528 This study was supported in part by a grant from the National Institutes of Health (NIH;
529 5R21AI144571-03, R01AI173084-03 and 1R01AI175461-01A1) and by a grant from NIGMS
530 through the Molecular Center of Health and Disease (1P20GM144041-01A1 7651). Studies of
531 confocal microscopy, and histology, were supported by grants from the National Institute of
532 General Medical Sciences (NIGMS) of the National Institutes of Health under Award Numbers
533 P20GM121334 and P20GM104357. The content is solely the responsibility of the authors and
534 does not necessarily represent the official view of the NIH.

535

536 **Authors' contributions**

537 A.G.J.V.- Formal analysis, Investigation, Supervision, Methodology, Project administration,
538 Writing - review & editing.

539 M.F. - Formal analysis, Investigation.

540 M.C.- Investigation.

541 I.J.F.- Investigation.

542 P.S. - Investigation.

543 P.V.- Investigation.

544 C.F. L.- Investigation, Methodology, Writing- review & editing.

545 C.G. - Investigation, Methodology, Writing - review & editing.

2-Oct-24

546 W.D. - Investigation.

547 J.E.V. -Conceptualization, Data curation, Formal analysis, Funding acquisition, Investigation,

548 Writing - original draft, Writing - review & editing.

549 All authors read and approved the final manuscript.

550 **Acknowledgements.** We thank Dr. Babek Alibayov from the University of Mississippi Medical

551 Center (UMMC) for their assistance with labeling aliquots of Spn-FLUO, and Dr. Kenichi

552 Takeshita, and Dr. Antonino Baez, also from UMMC, for their feedback on the manuscript. The

553 authors also acknowledge the assistance of Dr. Fuminori Sakai from Emory University Rollins

554 School of Public Health, currently at Pfizer Japan, for performing some qPCR assays.

555

556 **References**

557

558 1. Wahl, B. *et al.* Burden of *Streptococcus pneumoniae* and *Haemophilus influenzae* type b disease
559 in children in the era of conjugate vaccines: global, regional, and national estimates for 2000-15.
560 *Lancet Glob Health* **6**, e744-e757 (2018).

561

562 2. Weiser, J.N., Ferreira, D.M. & Paton, J.C. *Streptococcus pneumoniae*: transmission, colonization
563 and invasion. *Nat Rev Microbiol* **16**, 355-367 (2018).

564

565 3. Musher, D.M. & Thorner, A.R. Community-acquired pneumonia. *N Engl J Med* **371**, 1619-1628
566 (2014).

567

568 4. Ganaie, F. *et al.* A New Pneumococcal Capsule Type, 10D, is the 100th Serotype and Has a Large
569 cps Fragment from an Oral *Streptococcus*. *mBio* **11** (2020).

570

571 5. Brissac, T. *et al.* Capsule Promotes Intracellular Survival and Vascular Endothelial Cell
572 Translocation during Invasive Pneumococcal Disease. *mBio* **12**, e0251621 (2021).

573

2-Oct-24

- 574 6. Hyams, C., Camberlein, E., Cohen, J.M., Bax, K. & Brown, J.S. The Streptococcus pneumoniae
575 capsule inhibits complement activity and neutrophil phagocytosis by multiple mechanisms.
576 *Infect Immun* **78**, 704-715 (2010).
577
- 578 7. Kim, J.O. *et al.* Relationship between cell surface carbohydrates and intrastrain variation on
579 opsonophagocytosis of Streptococcus pneumoniae. *Infect Immun* **67**, 2327-2333 (1999).
580
- 581 8. Miller, J.M. *et al.* A Guide to Utilization of the Microbiology Laboratory for Diagnosis of
582 Infectious Diseases: 2018 Update by the Infectious Diseases Society of America and the
583 American Society for Microbiology. *Clin Infect Dis* **67**, e1-e94 (2018).
584
- 585 9. Pletz, M.W. *et al.* Unmet needs in pneumonia research: a comprehensive approach by the
586 CAPNETZ study group. *Respir Res* **23**, 239 (2022).
587
- 588 10. Walker, A.M., Timbrook, T.T., Hommel, B. & Prinzi, A.M. Breaking Boundaries in Pneumonia
589 Diagnostics: Transitioning from Tradition to Molecular Frontiers with Multiplex PCR. *Diagnostics*
590 (*Basel*) **14** (2024).
591
- 592 11. Marimuthu, S., Damiano, R.B. & Wolf, L.A. Performance Characteristics of a Real-Time PCR Assay
593 for Direct Detection of Streptococcus pneumoniae in Clinical Specimens. *J Mol Diagn* **26**, 552-
594 562 (2024).
595
- 596 12. Carvalho Mda, G. *et al.* Evaluation and improvement of real-time PCR assays targeting *lytA*, *ply*,
597 and *psaA* genes for detection of pneumococcal DNA. *J Clin Microbiol* **45**, 2460-2466 (2007).
598
- 599 13. Wyllie, A.L. *et al.* Streptococcus pneumoniae in saliva of Dutch primary school children. *PLoS*
600 *One* **9**, e102045 (2014).
601
- 602 14. Tavares, D.A. *et al.* Identification of Streptococcus pneumoniae by a real-time PCR assay
603 targeting SP2020. *Sci Rep* **9**, 3285 (2019).
604
- 605 15. Shkodenko, L.A., Mohamed, A.A., Ateiah, M., Rubel, M.S. & Koshel, E.I. A DAMP-Based Assay for
606 Rapid and Affordable Diagnosis of Bacterial Meningitis Agents: Haemophilus influenzae,
607 Neisseria meningitidis, and Streptococcus pneumoniae. *Int J Mol Sci* **25** (2024).
608
- 609 16. Gotts, J.E. *et al.* Clinically relevant model of pneumococcal pneumonia, ARDS, and
610 nonpulmonary organ dysfunction in mice. *Am J Physiol Lung Cell Mol Physiol* **317**, L717-L736
611 (2019).
612
- 613 17. Lee, J.S., Giesler, D.L., Gellad, W.F. & Fine, M.J. Antibiotic Therapy for Adults Hospitalized With
614 Community-Acquired Pneumonia: A Systematic Review. *JAMA* **315**, 593-602 (2016).

2-Oct-24

- 615
616 18. Wu, X. *et al.* Effect of pneumococcal conjugate vaccine availability on Streptococcus
617 pneumoniae infections and genetic recombination in Zhejiang, China from 2009 to 2019. *Emerg*
618 *Microbes Infect* **11**, 606-615 (2022).
- 619
620 19. Viteri-Davila, C. *et al.* The Crisis of Macrolide Resistance in Pneumococci in Latin America. *Am J*
621 *Trop Med Hyg* (2024).
- 622
623 20. Tettelin, H. *et al.* Complete genome sequence of a virulent isolate of Streptococcus pneumoniae.
624 *Science* **293**, 498-506 (2001).
- 625
626 21. Wu, X. *et al.* Interaction between Streptococcus pneumoniae and Staphylococcus aureus
627 Generates (.)OH Radicals That Rapidly Kill Staphylococcus aureus Strains. *J Bacteriol* **201** (2019).
- 628
629 22. McDevitt, E. *et al.* Hydrogen Peroxide Production by Streptococcus pneumoniae Results in
630 Alpha-hemolysis by Oxidation of Oxy-hemoglobin to Met-hemoglobin. *mSphere* **5** (2020).
- 631
632 23. Lanie, J.A. *et al.* Genome sequence of Avery's virulent serotype 2 strain D39 of Streptococcus
633 pneumoniae and comparison with that of unencapsulated laboratory strain R6. *J Bacteriol* **189**,
634 38-51 (2007).
- 635
636 24. Junges, R., Maienschein-Cline, M., Morrison, D.A. & Petersen, F.C. Complete Genome Sequence
637 of Streptococcus pneumoniae Serotype 19F Strain EF3030. *Microbiol Resour Announc* **8** (2019).
- 638
639 25. Wu, X. *et al.* Competitive Dominance within Biofilm Consortia Regulates the Relative Distribution
640 of Pneumococcal Nasopharyngeal Density. *Appl Environ Microbiol* **83** (2017).
- 641
642 26. Wu, X. *et al.* Ultrastructural, metabolic and genetic characteristics of determinants facilitating
643 the acquisition of macrolide resistance by Streptococcus pneumoniae. *Drug Resist Updat* **77**,
644 101138 (2024).
- 645
646 27. Alibayov, B. *et al.* Oxidative Reactions Catalyzed by Hydrogen Peroxide Produced by
647 Streptococcus pneumoniae and Other Streptococci Cause the Release and Degradation of Heme
648 from Hemoglobin. *Infect Immun* **90**, e0047122 (2022).
- 649
650 28. Sakai, F., Sonaty, G., Watson, D., Klugman, K.P. & Vidal, J.E. Development and characterization of
651 a synthetic DNA, NUversa, to be used as a standard in quantitative polymerase chain reactions
652 for molecular pneumococcal serotyping. *FEMS Microbiol Lett* **364** (2017).
- 653

2-Oct-24

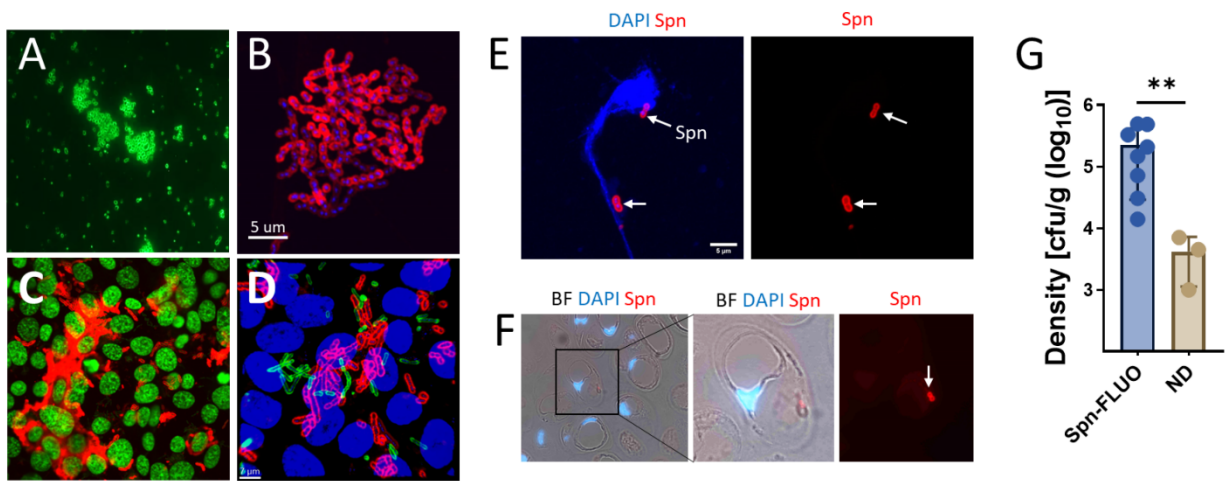
- 654 29. Pholwat, S., Sakai, F., Turner, P., Vidal, J.E. & Houpt, E.R. Development of a TaqMan Array Card
655 for Pneumococcal Serotyping on Isolates and Nasopharyngeal Samples. *J Clin Microbiol* **54**,
656 1842-1850 (2016).
- 657
- 658 30. Chien, Y.W. *et al.* Density interactions among *Streptococcus pneumoniae*, *Haemophilus*
659 *influenzae* and *Staphylococcus aureus* in the nasopharynx of young Peruvian children. *Pediatr*
660 *Infect Dis J* **32**, 72-77 (2013).
- 661
- 662 31. Grijalva, C.G. *et al.* Cohort profile: The study of respiratory pathogens in Andean children. *Int J*
663 *Epidemiol* **43**, 1021-1030 (2014).
- 664
- 665 32. Howard, L.M. *et al.* Association between nasopharyngeal colonization with multiple
666 pneumococcal serotypes and total pneumococcal colonization density in young Peruvian
667 children. *Int J Infect Dis* **134**, 248-255 (2023).
- 668
- 669 33. Nelson, K.N. *et al.* Dynamics of Colonization of *Streptococcus pneumoniae* Strains in Healthy
670 Peruvian Children. *Open Forum Infect Dis* **5**, ofy039 (2018).
- 671
- 672 34. Satzke, C. *et al.* Standard method for detecting upper respiratory carriage of *Streptococcus*
673 *pneumoniae*: updated recommendations from the World Health Organization Pneumococcal
674 Carriage Working Group. *Vaccine* **32**, 165-179 (2013).
- 675
- 676 35. O'Brien, K.L. *et al.* Evaluation of a medium (STGG) for transport and optimal recovery of
677 *Streptococcus pneumoniae* from nasopharyngeal secretions collected during field studies. *J Clin*
678 *Microbiol* **39**, 1021-1024 (2001).
- 679
- 680 36. Sakai, F., Talekar, S.J., Klugman, K.P. & Vidal, J.E. Expression of Virulence-Related Genes in the
681 Nasopharynx of Healthy Children. *PloS one* **8**, e67147 (2013).
- 682
- 683 37. Centers for Disease Control and Prevention & (CDC). *Streptococcus pneumoniae* carriage study
684 protocol - nasopharyngeal (NP) swab processing.; 2010.
- 685
- 686 38. Leber, A.L. *Clinical microbiology procedures handbook*, 4th edition. edn. ASM Press: Washington,
687 DC, 2016.
- 688
- 689 39. Scott, E.J., 2nd, Luke-Marshall, N.R., Campagnari, A.A. & Dyer, D.W. Draft Genome Sequence of
690 Pediatric Otitis Media Isolate *Streptococcus pneumoniae* Strain EF3030, Which Forms In Vitro
691 Biofilms That Closely Mimic In Vivo Biofilms. *Microbiol Resour Announc* **8** (2019).
- 692
- 693 40. Vidal, J.E. *et al.* Prophylactic inhibition of colonization by *Streptococcus pneumoniae* with the
694 secondary bile acid metabolite deoxycholic acid. *Infect Immun*, IA10046321 (2021).

2-Oct-24

- 695
696 41. Vidal, J.E. *et al.* Prophylactic Inhibition of Colonization by *Streptococcus pneumoniae* with the
697 Secondary Bile Acid Metabolite Deoxycholic Acid. *Infect Immun* **89**, e0046321 (2021).
- 698
699 42. Hanke, C.R. *et al.* Bacterial Density, Serotype Distribution and Antibiotic Resistance of
700 Pneumococcal Strains from the Nasopharynx of Peruvian Children Before and After
701 Pneumococcal Conjugate Vaccine 7. *Pediatr Infect Dis J* **35**, 432-439 (2016).
- 702
703 43. Echlin, H., Frank, M., Rock, C. & Rosch, J.W. Role of the pyruvate metabolic network on
704 carbohydrate metabolism and virulence in *Streptococcus pneumoniae*. *Mol Microbiol* **114**, 536-
705 552 (2020).
- 706
707 44. Alibayov, B. *et al.* Oxidation of hemoglobin in the lung parenchyma facilitates the differentiation
708 of pneumococci into encapsulated bacteria. *bioRxiv* (2023).
- 709
710 45. Esther, C.R., Jr. *et al.* Sialic acid-to-urea ratio as a measure of airway surface hydration. *Am J*
711 *Physiol Lung Cell Mol Physiol* **312**, L398-L404 (2017).
- 712
713 46. Calvo-Silveria, S. *et al.* Evolution of invasive pneumococcal disease by serotype 3 in adults: a
714 Spanish three-decade retrospective study. *Lancet Reg Health Eur* **41**, 100913 (2024).
- 715
716 47. Riccobono, E., Bussini, L., Giannella, M., Viale, P. & Rossolini, G.M. Rapid diagnostic tests in the
717 management of pneumonia. *Expert Rev Mol Diagn* **22**, 49-60 (2022).
- 718
719 48. Keller, L.E., Robinson, D.A. & McDaniel, L.S. Nonencapsulated *Streptococcus pneumoniae*:
720 Emergence and Pathogenesis. *mBio* **7**, e01792 (2016).
- 721
722
723
724
725
726
727
728
729
730

2-Oct-24

731 **Figure legends**



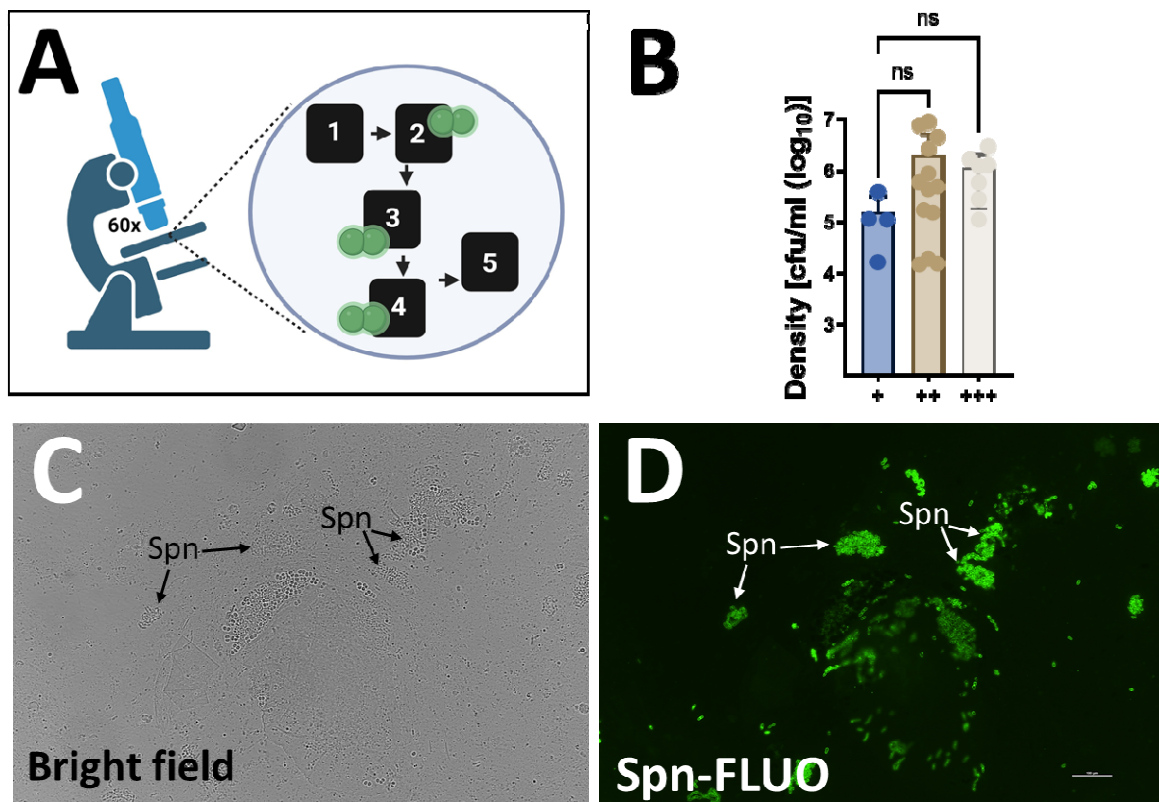
732

733 **Figure 1. *In vitro* and *in vivo* detection of pneumococci with fluorescently-labelled antibodies.**

734 Strain TIGR4 (A) was mixed with anti S4-A488 (green) antibody and observed under a
735 epifluorescence microscope within five minutes. (B) Spn serotype 19F strain 4924 was cultured
736 for four h in a 8-well slide and pneumococci attached to the substratum were stained with an
737 anti S19-A555 (red) antibody and the DNA was stained with DAPI. (C-D) Human pharyngeal cells
738 grown to confluence were inoculated with (C) strain D39 or (D) a mixture of strain D39 and
739 strain TIGR4 and incubated for four hours. D39 was stained with S2-A555 (red) and TIGR4 was
740 stained with S4-A488. In panel C, DNA was stained with TO-PRO-3, while in panel D, it was
741 stained with DAPI. (E-F) C57BL/6 mice (N=11) were intranasally inoculated with serotype 19F
742 strain EF3030. After 48 h, mice were euthanized, and the nasal bone was removed.
743 Nasopharyngeal tissue was collected, sectioned (~5 μm), or homogenized. Nasopharyngeal
744 homogenate (E) or tissue sections (F) were stained with DAPI and with an anti S19-A555
745 antibody. Arrows point out Spn. In panels B-F, micrographs were obtained by confocal
746 microscopy, and the projection of z-stacks is shown. (G) Nasopharyngeal homogenates were

2-Oct-24

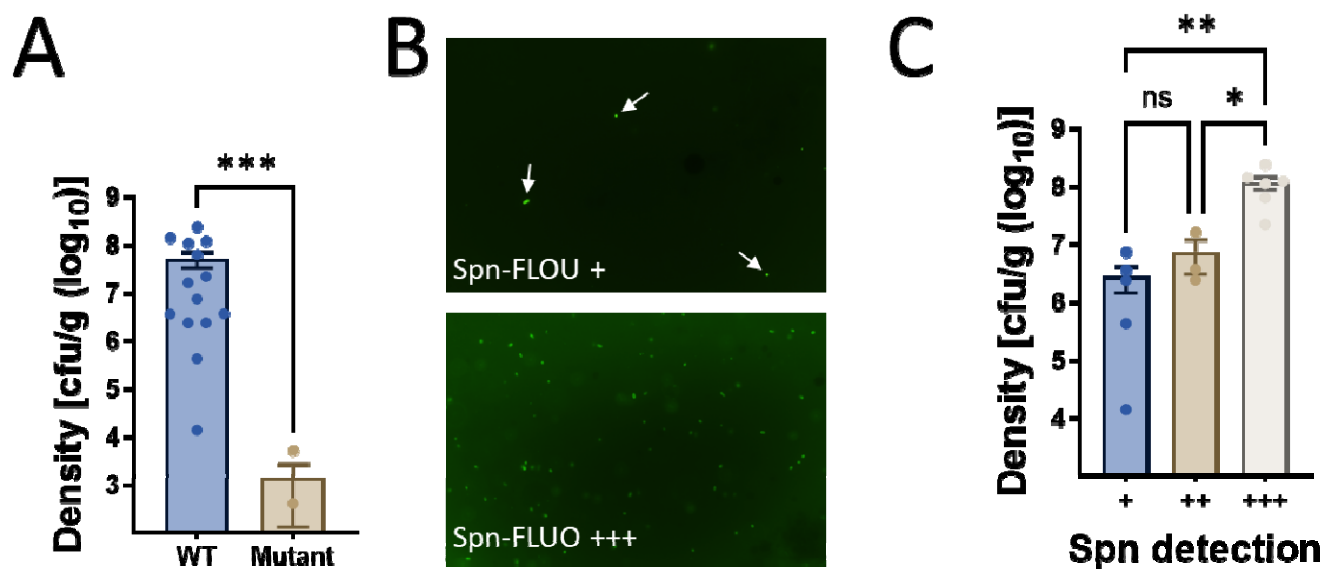
747 diluted and plated to obtain the bacterial density. The density in the plot was grouped
748 according to whether the samples yielded a positive reaction with Spn-FLUO or were not
749 detected (ND). Student t test, $**p=0.01$.



750
751 **Figure 2. Detection of *S. pneumoniae* with Spn-FLUO in human specimens.** (A) Detection
752 algorithm for the identification of Spn in clinical specimens. Five fields were screened using the
753 60x objective, and a specimen was scored positive when ≥ 1 to < 5 (+), ≥ 5 to < 10 (++) or ≥ 10
754 (+++) pneumococci were observed in at least three fields. This algorithm was chosen to ensure
755 the reliable detection of Spn while minimizing the risk of false positives. (B) The density of *S.*
756 *pneumoniae* in nasopharyngeal specimens that yielded a positive reaction with Spn-FLUO was
757 categorized depending on the semiquantitative algorithm. Data are presented as mean \pm SD.

2-Oct-24

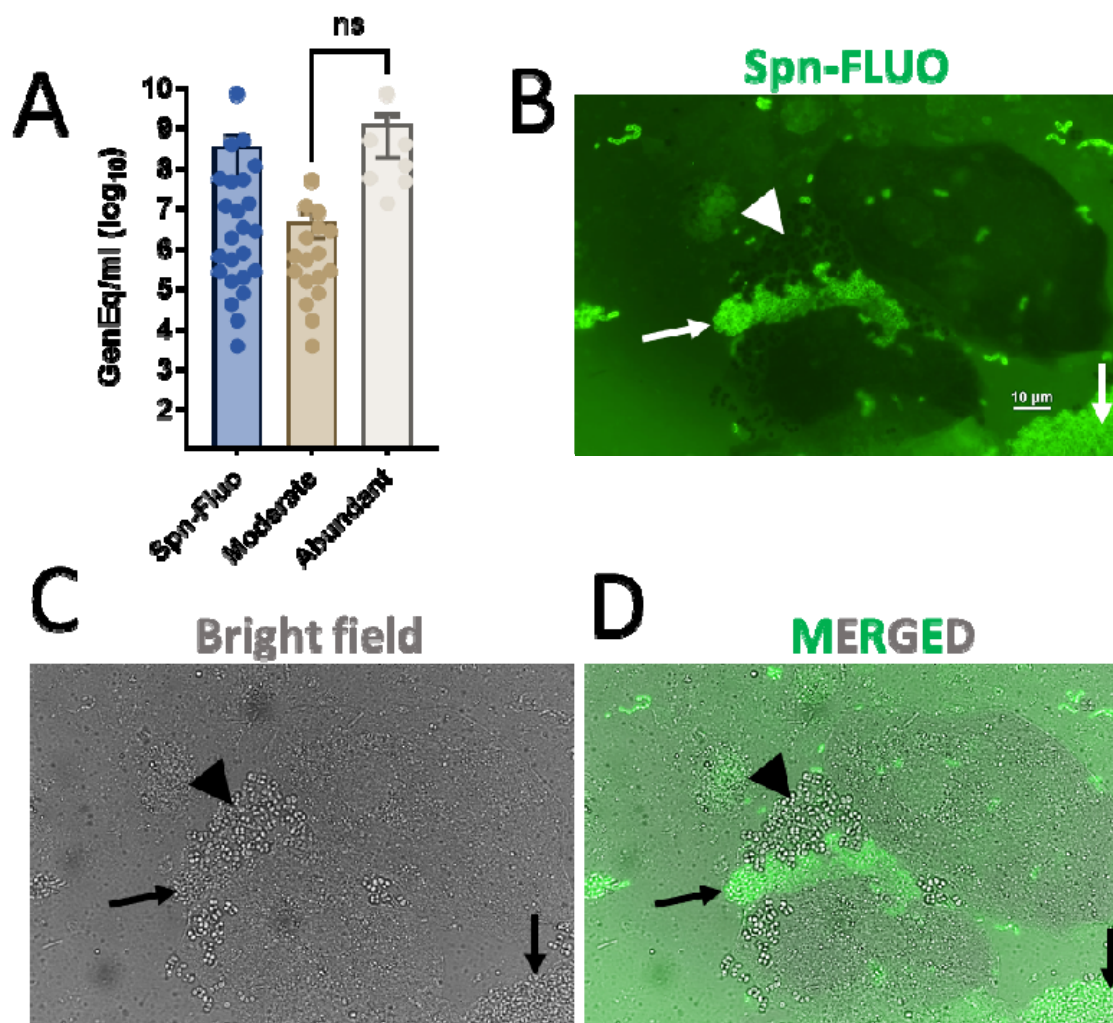
758 Differences in bacterial density were determined using one-way ANOVA followed by Dunnett's
759 multiple comparisons test. ns=no significant difference. (C-D) Sputum specimen stained with
760 Spn-FLUO and observed under (C) bright field and (D) epifluorescence in the green channel.
761 Arrows point out Spn identified by Spn-FLUO.
762



763
764 **Figure 3. Detection of *S. pneumoniae* with Spn-FLUO in mouse lung specimens.** Balb/c mice
765 were intranasally inoculated with strain TIGR4 or isogenic mutant $\Delta spxB\Delta ctO$ and euthanized
766 when deemed moribund, or after 96 h post-infection. Lungs were collected and homogenized.
767 (A) Lung homogenates were diluted and plated to obtain the bacterial density. (B) Aliquots of
768 lung homogenate were stained with Spn-FLUO and scored for the presence of pneumococci.
769 Micrographs were obtained with a fluorescence microscope in the green channel. The top panel
770 shows a representative specimen scored “+” with arrows pointing out *S. pneumoniae*, while the
771 bottom panel shows a representative specimen that scored “+++”. (C) The density in the

2-Oct-24

772 graphic was grouped according to the semiquantitative detection of *S. pneumoniae* with Spn-
773 FLUO. Statistical significance of differences in bacterial density were determined using
774 Student's t-test (A) or one-way ANOVA followed by Dunnett's multiple comparisons test (C).
775 * $p=0.027$, ** $p=.0088$, *** $p=0.0007$.
776

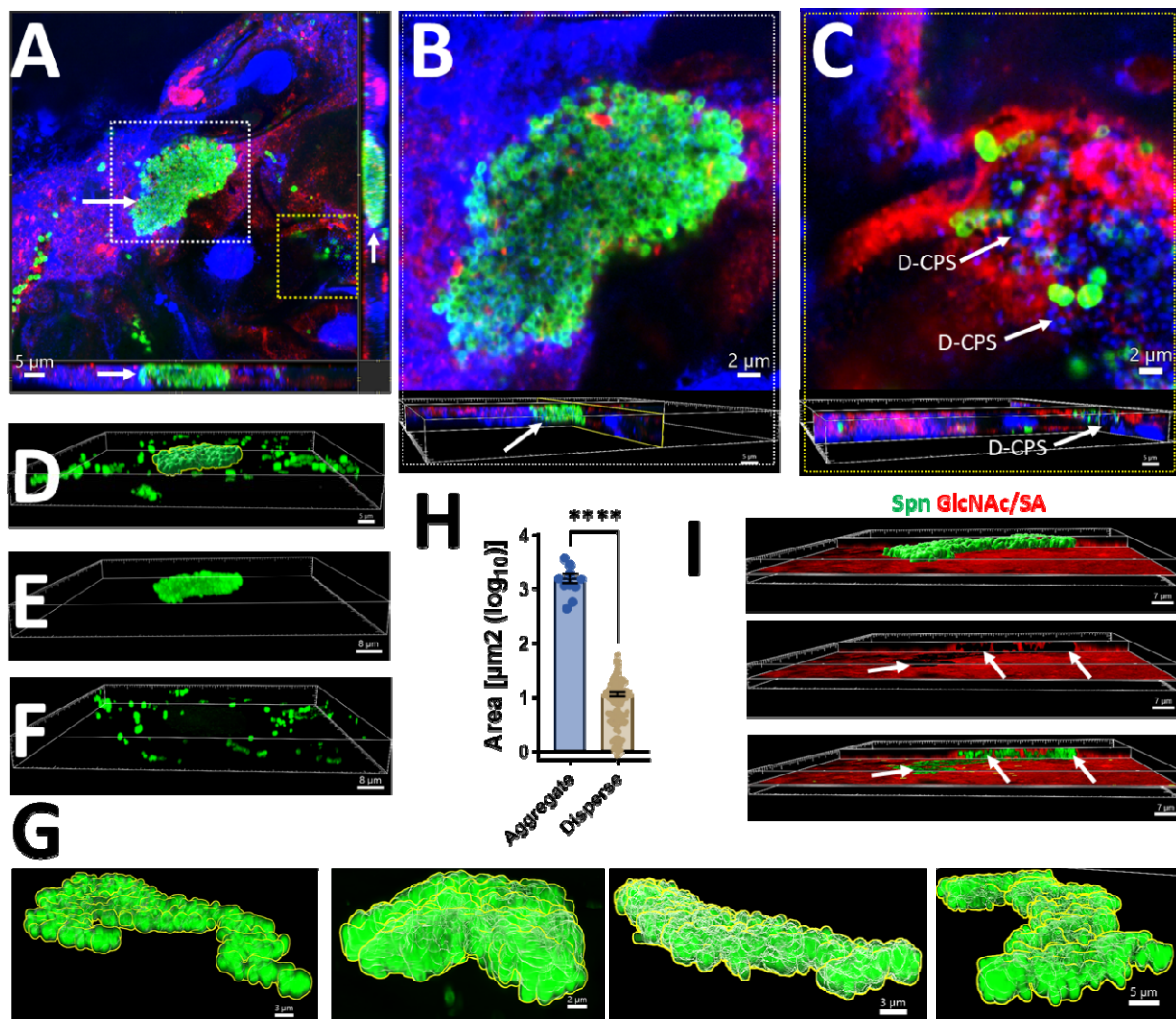


777
778 **Figure 4. Detection of *S. pneumoniae* with Spn-FLUO in human sputum.** (A) Aliquots of sputum
779 were DNA extracted and used as templates in qPCR reactions targeting the *lytA* gene. Other
780 aliquots were stained with Spn-FLUO, and the presence of *S. pneumoniae* was scored. The

2-Oct-24

781 graphic shows the pneumococcal genome equivalent (GenEq)/ml in all samples, categorized as
782 low (scored +), medium (scored ++), or high (scored +++). Statistical significance of differences
783 in bacterial density was assessed using the Student's t-test. ns=no significant difference. (B-D)
784 Sputum specimens stained with Spn-FLUO and observed under (B) epifluorescence in the green
785 channel or (C) bright field. Panel (D) shows the merged epifluorescence and bright field
786 channels. Arrows point out *S. pneumoniae* identified by Spn-FLUO, while arrowheads signal
787 staphylococcus-like microcolonies, which were not stained by Spn-FLUO but were observed in
788 the bright field channels.
789

2-Oct-24



790

791

792 **Figure 5. Ultrastructural analysis of *S. pneumoniae* in human sputum.** Sputum specimens were

793 stained with Spn-FLUO (green), wheat germ agglutinin (WGA) labeled with Alexa 555 (red), and

794 DNA was stained with DAPI (blue). Preparations were analyzed by confocal microscopy. Panel

795 (A) shows middle XY, XZ (bottom), and YZ (side) optical sections. The white inset indicates an

796 optical zoom shown in panel (B), while the yellow inset indicates the region shown in panel (C).

797 The bottom panels in (B and C) show orthogonal XZ and YZ sections. Decapsulated pneumococci

798 (D-CPS) are indicated by the arrows. (D-F) A mask was created in the green channel (D) to

2-Oct-24

799 analyze the 3D structure of the pneumococcal (E) aggregate or (F) dispersed pneumococci. (G)
800 Representative 3D images of aggregated pneumococci across the sputum specimen,
801 showcasing their size, shape, and spatial distribution within the sputum. (H) The area of those
802 aggregate pneumococci and that of dispersed bacteria was plotted. Student's t-test was
803 performed to assess statistical significance, **** $p < 0.0001$. (I) Orthogonal XY and YZ sections
804 were created using the green (Spn-FLUO) and the red channel (WGA). WGA binds acetyl
805 glucosamine and sialic acid residues (GlcNAc/SA). The top panel shows the masked green
806 channel representing the area of the pneumococcal aggregate. The pneumococcal aggregate
807 was removed from the middle panel to reveal the hollow spaces occupied by bacteria
808 embedded in the sputum. The bottom panel shows the non-masked green channel and the red
809 channel. All analyses were performed using the Imaris software.
810

2-Oct-24

811 Table 1. Detection of pneumococci using Spn-FLUO in the upper respiratory tract of mice.

Mouse nasopharynx	Density (cfu/organ)	Spn-FLUO*	S19-A555*
MN-1	7.1×10^3	ND	ND
MN-2	3.27×10^5	+	+
MN-3	4.93×10^5	+	+
MN-4	1.4×10^4	+	+
MN-5	1.47×10^5	+	+
MN-6	4.83×10^5	+	+
MN-7	1.0×10^3	ND	ND
MN-8	4.5×10^3	ND	ND
MN-9	7.2×10^4	+	+
MN-10	3.07×10^4	+	+
MN-11	2.09×10^5	+	+

812 *ND=not detected.

813 +, up to five pneumococci per field in at least three fields of five observed using
814 the 60x objective.

815

2-Oct-24

816 **Table 2. Detection of Spn in nasopharyngeal specimens from children with Spn-**
817 **FLUO.**

818

Nasopharyngeal specimen	qPCR (GenEq/ml) [#]	Spn-FLUO*
HN-1	5.73E+05	+++
HN-2	1.67E+06	+++
HN-3	1.61E+04	+
HN-4	2.60E+06	++
HN-5	1.46E+04	++
HN-6	4.47E+06	++
HN-7	1.20E+06	+++
HN-8	1.49E+05	++
HN-9	4.70E+05	++
HN-10	2.72E+05	+++
HN-11	1.75E+04	ND
HN-12	1.51E+04	++
HN-13	1.26E+06	+++
HN-14	5.83E+05	++
HN-15	1.08E+05	+++
HN-16	1.87E+04	++
HN-17	8.65E+05	++
HN-18	2.92E+06	+++
HN-19	3.81E+05	+
HN-20	1.67E+05	++
HN-21	4.18E+05	++
HN-22	1.08E+05	+
HN-23	1.12E+05	+
HN-24	7.64E+06	++
HN-25	8.88E+06	++
HN-26 to HN-50	Negative	Negative

819 [#]*lytA*-based qPCR assay. ND=not detected.

820

821

822

2-Oct-24

823 Table 3. Detection of pneumococci using Spn-FLUO in the lung of mice.

Mouse (strain)	Density (cfu/ml)	Spn-FLUO
ML-1 (TIGR4)	6.25E+07	+++
ML-2 (TIGR4)	2.39E+08	+++
ML-3 (TIGR4)	1.39E+04	+
ML-4 (TIGR4)	2.38E+06	++
ML-5 (TIGR4)	1.09E+08	+++
ML-6 (TIGR4)	4.23E+05	+
ML-7 (Δ <i>spxB</i> Δ <i>ctO</i>)	5.28E+03	ND
ML-8 (Δ <i>spxB</i> Δ <i>ctO</i>)	4.03E+02	ND
ML-9 (TIGR4)	2.35E+06	+
ML-10 (TIGR4)	3.60E+06	+
ML-11 (TIGR4)	7.40E+06	+
ML-12 (Δ <i>spxB</i> Δ <i>ctO</i>)	0.00E+00	ND
ML-13 (Δ <i>spxB</i> Δ <i>ctO</i>)	0.00E+00	ND
ML-14 (TIGR4)	1.21E+08	+++
ML-15 (TIGR4)	1.41E+08	+++
ML-16 (TIGR4)	1.62E+07	+++
ML-18 (TIGR4)	2.18E+07	+++
ML-19 (TIGR4)	3.64E+06	++

824

825

826

827

828

829

830

831

832

833

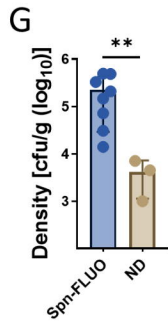
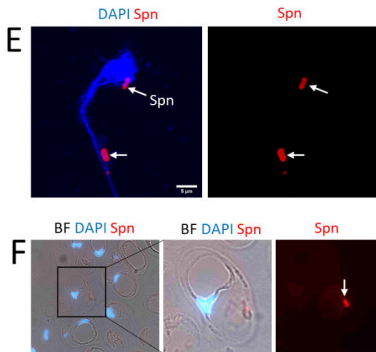
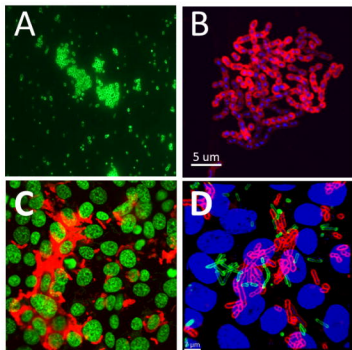
834

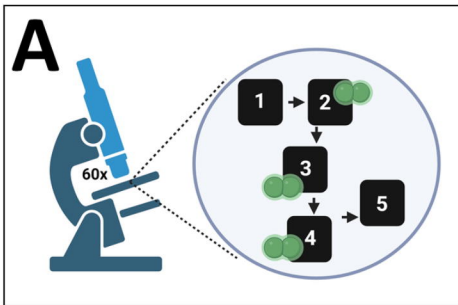
2-Oct-24

835 **Table 4. Detection of Spn in culture-positive specimen from patients with pneumococcal pneumonia**
 836 **using Spn-FLUO.**

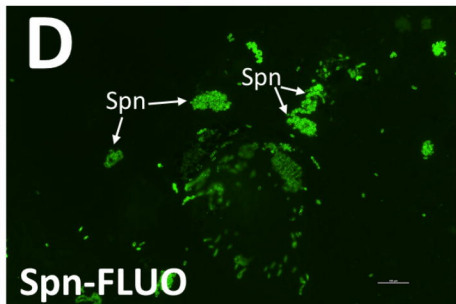
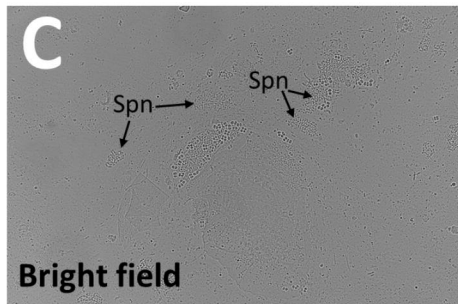
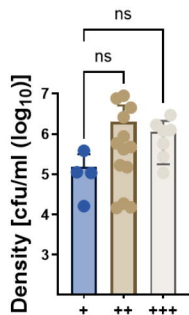
Specimen	ID	Specimen	qPCR (GE/ml)*	Spn-FLUO
HL1	082W	Sputum	3.25x10 ⁶	+
HL2	U019	BAL ^{&} (endotracheal Tube)	5.45x10 ⁷	+++
HL3	U0134	Sputum	6.16x10 ⁵	+
HL4	U146	Sputum	5.10x10 ⁵	+
HL5	U265	Sputum	3.63x10 ³	+
HL6	U2275	BAL (endotracheal Tube)	ND	+++
HL7	U6831	BAL (endotracheal Tube)	7.29x10 ⁹	+
HL8	U077	Sputum	2.73x10 ⁵	+
HL9	U097	Sputum	1.84x10 ⁵	+
HL10	U260	Sputum	1.81x10 ⁶	+
HL11	U227.46	BAL (endotracheal Tube)	4.85x10 ⁸	+++
HL12	U080	Sputum	1.10x10 ⁷	+
HL13	U081	Sputum	1.31x10 ⁷	++++
HL14	U081-W	Sputum	7.54x10 ⁴	+
HL15	U220	Sputum	2.60x10 ⁵	+
HL16	U766	Sputum	6.36x10 ⁵	-
HL17	U156	Sputum	7.56x10 ⁵	+
HL18	U209	Sputum	2.67x10 ⁶	+
HL19	U210	Sputum	5.32x10 ⁴	-
HL20	U501	Sputum	3.95x10 ⁴	++
HL21	UC1	Sputum	5.06x10 ⁷	++
HL22	UC2	Throat swab	1.48.x10 ⁵	++
HL23	UC3	Throat swab	1.57x10 ⁴	+
HL24	UC4	Sputum	4.57x10 ⁷	++++
HL25	UC4	Endotracheal aspirate	1.13x10 ⁸	++++
HL26	UC5	BAL (endotracheal tube)	3.84x10 ⁸	+++
HL27	UE1	BAL (endotracheal tube)	8.19x10 ⁶	++

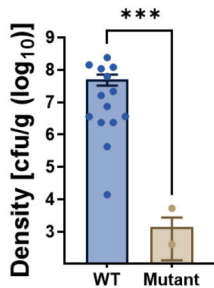
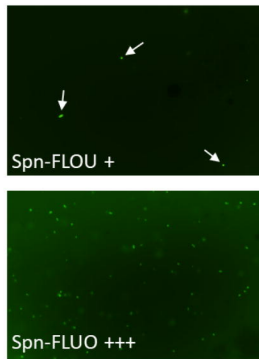
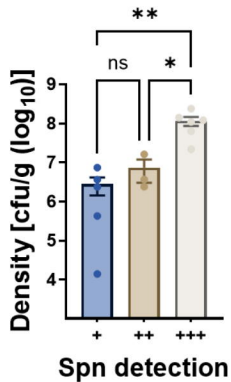
837 *Genome equivalent/ml; [&]Bronchoalveolar lavage,

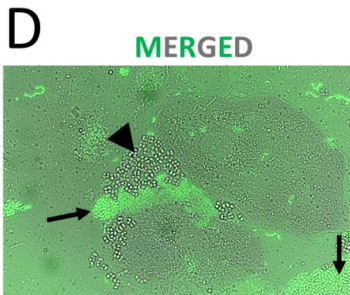
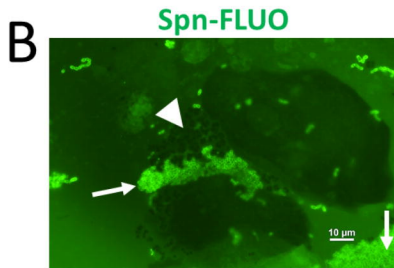
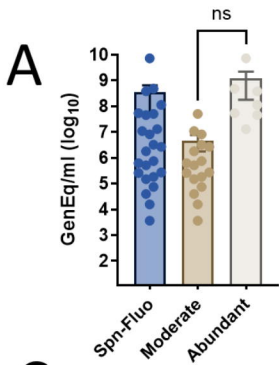


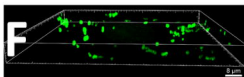
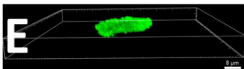
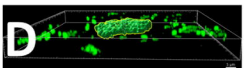
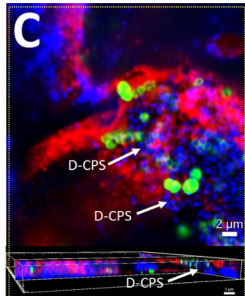
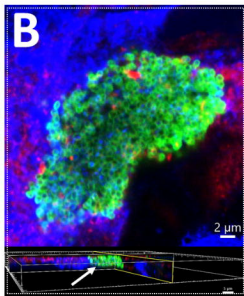
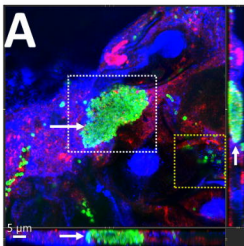


B

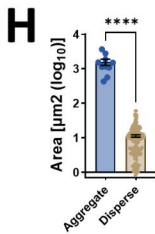
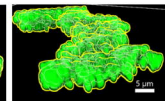
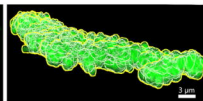
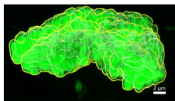
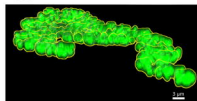


A**B****C**





G



I

